

Search for doubly charged Higgs bosons through VBF at the LHC, and beyond

G. Bambhaniya*

Theoretical Physics Division, Physical Research Laboratory, Ahmedabad-380009, India

J. Chakraborty†

Department of Physics, Indian Institute of Technology, Kanpur-208016, India

J. Gluza‡ and T. Jeliński§

Institute of Physics, University of Silesia, Uniwersytecka 4, 40-007 Katowice, Poland

R. Szafron¶

Department of Physics, University of Alberta, Edmonton, AB T6G 2E1, Canada

Production and decays of doubly charged Higgs bosons at the LHC and future hadron colliders triggered by vector boson fusion mechanism are discussed in the context of the Minimal Left-Right Symmetric Model. Our analysis is based on the Higgs boson mass spectrum compatible with available constraints which include FCNC effects and vacuum stability of the scalar potential. Though the parity breaking scale v_R is large (\sim few TeV) and scalar masses which contribute to FCNC effects are even larger, consistent Higgs boson mass spectrum still allows us to keep doubly charged scalar masses below 1 TeV which is an interesting situation for LHC and future FCC colliders. We have shown that allowed Higgs bosons mass spectrum constrains the splittings ($M_{H_1^{\pm\pm}} - M_{H_1^{\pm}}$), closing the possibility of $H_1^{\pm\pm} \rightarrow W_1^{\pm} H_1^{\pm}$ decays. Assuming that doubly charged Higgs bosons decay predominantly into a pair of same sign charged leptons through the process $pp \rightarrow H_{1/2}^{\pm\pm} H_{1/2}^{\mp\mp} jj \rightarrow \ell^{\pm} \ell^{\pm} \ell^{\mp} \ell^{\mp} jj$, we find that for LHC operating at $\sqrt{s} = 14$ TeV with an integrated luminosity at the level of 3000 fb^{-1} (HL-LHC) there is practically no chance to detect such particles at the reasonable significance level through this channel. However, 33 TeV HE-LHC and (or) 100 TeV FCC-hh open up a wide region for doubly charged Higgs boson mass spectrum to be explored. In FCC-hh, doubly charged Higgs bosons mass up to 1 TeV can be probed easily.

PACS numbers: 12.60.-i, 12.60.Fr, 14.80.Fd, 14.80.Ec

I. INTRODUCTION

Weak vector boson fusion (VBF) processes have been suggested quite some time ago in the context of Higgs searches [1–3]. They are characterized by the presence of two jets with large transverse momentum (p_T) in the forward region in opposite hemispheres along with other observables, like charged leptons. In fact, many interesting Standard Model (SM) processes, e.g. diffractive interactions, low-x QCD physics, VBF Higgs production, photo-production are also accompanied by production of forward particles. Interestingly LHC has a very rich “forward physics” program and for the necessary investigation there are dedicated detectors like LHCf [4] and (or) FP420 [5]. Due to uncertainties in jet tagging the efficiency is relatively low and thus the significance of these channels are rather suppressed. But nevertheless from the discovery perspective, many Beyond Standard Mod-

els (BSM) can also be tested using forward jets. Such related studies are also important for dark matter searches through mono-jet plus missing energy [6–8].

In this paper we continue [9–11] a dedicated analysis of the Minimal Left-Right Symmetric Model (MLRSM) [12–14] aiming at exhaustive exploration of interesting BSM signals at present and future hadron colliders¹. For many reasons parity breaking scale v_R of the right $SU(2)$ group in MLRSM must be already around $\mathcal{O}(10)$ TeV [9–11, 18, 19]. However, as discussed recently in [10, 11], in such models charged Higgs bosons can have masses at a much lower level of a few hundred GeV and that scenario is still consistent with experimental data. In this case it is imperative to cover all possible scenarios and their potential effects at the LHC should be analyzed carefully. Interestingly enough, recent CMS study [20] can be interpreted at the favour of right handed currents.

In our previous analyses we have worked with the scalar mass spectra which are compatible with unitarity of the potential parameters, large parity breaking

* gulab@prl.res.in

† joydeep@iitk.ac.in

‡ janusz.gluza@us.edu.pl

§ tomasz.jelinski@us.edu.pl

¶ szafron@ualberta.ca

¹ The main features of this model are equal $SU(2)$ left and right gauge couplings, $g_L = g_R$, and a scalar potential which contains a bidoublet and two triplet scalar multiplets, considered for the first time in [15], see also [16, 17].

scale v_R and severe bounds on neutral scalar masses ($M_{H_1^0}, M_{A_1^0}$) derived from Flavor Changing Neutral Current (FCNC). In this work we have further implemented another necessary condition: vacuum stability of the scalar potential. It appears that even after taking into account all these constraints, the consistent scalar mass spectra can accommodate doubly charged Higgs boson masses in a region which can be explored by the LHC.

In past, we have focused on searches for multi-lepton signals associated with any number of jets, i.e., there was no jet veto. Here, the analysis of possible VBF-type signals with four leptons and two jets using suitable VBF cuts are discussed.

We have used our version of the Left-Right symmetric model implemented in FeynRules (v2.0.31) [21, 22]. The general signal and background analyses for multi-lepton and tagged forward jets are performed using ALPGEN (v2.14) [23], Madgraph (v2.2.2) [24] and PYTHIA (v6.421) [25].

II. POSSIBLE PROCESSES WHICH IDENTIFY DOUBLY CHARGED HIGGS THROUGH VBF IN MLRSM

There are many interesting channels in which doubly charged Higgs particles can be produced in MLRSM. In hadron collider, productions of doubly charged Higgs particles crucially depend on their couplings with vector bosons. These charged scalars ($H^{\pm\pm}$) are produced either through neutral and charged currents or fusion processes. Representative classes of diagrams which contribute to $H^{\pm\pm}$ productions associated with two jets are given in Fig. 1.

If $X = H^{\pm\pm}$ in Fig. 1 then doubly charged Higgs particles are produced in pairs. Assuming further that $H^{\pm\pm}$ decays predominantly into leptons, a signal of four leptons associated with two forward jets in the final state is foreseen, $pp \rightarrow H_{1/2}^{\pm\pm} H_{1/2}^{\mp\mp} jj \rightarrow \ell^\pm \ell^\pm \ell^\mp \ell^\mp jj$. In a Drell-Yan case also (diagram (d) in Fig. 1), if $X = H^{\pm\pm}$, four leptons plus two jets signal is possible, though its contribution is suppressed once the VBF cuts are activated.

We should also mention that vector boson fusion diagrams interfere substantially with Bremsstrahlung-like (or Drell-Yan) processes [26].

Here, we focus on the pair production of doubly charged scalars associated with two forward jets. As mentioned already this signature can be promising since LHC has dedicated search channels for tagged forward jets. VBF processes with doubly charged Higgs bosons have been considered lately in [27] with the main focus on three lepton signals with missing energy, and in [28] where doubly charged Higgs bosons decay into same-sign W bosons. In [27] there is also an interesting discussion on scalar self-energy corrections to W_L^\pm and $\Delta\rho_{EW}$ parameter. It has been argued that there exists severe constraints on the charged scalar mass splitting. However, in our opinion conclusions based on partial results and

single class of (scalar) diagrams can be deceptive thus we need to consider complete calculations including renormalization. We recall a series of papers on the 1-loop corrections to the muon decay in MLRSM, starting with qualitative results [29, 30] and finishing with quantitative analysis [31]. The upshot of all these analyses, important for our present discussion, is that there is a strong fine-tuning between contributions to $\Delta\rho_{EW}$ from different classes of non-standard particles: Higgs and additional gauge bosons and heavy neutrinos (fermions). By their nature, cancellations among bosonic and fermionic type of diagrams are present, and a change of mass spectrum of Higgs bosons can be compensated by different choices of v_R scale (gauge bosons) and masses of heavy neutrinos. These analyses in context of the LHC have been considered in details in [9].

III. CONSTRAINTS ON α_3 AND $\delta\rho$: ADDING VACUUM STABILITY CONDITION

Analysis of the LHC data provides lower limits on doubly charged Higgs mass [32] depending on their leptonic decay branching fractions. In the scenario where $\text{BR}(H^{++} \rightarrow e^+e^+) = \text{BR}(H^{++} \rightarrow \mu^+\mu^+) \approx 0.5$ that limit is $M_{\text{LHC}} = M_{H^{\pm\pm}} \approx 450 \text{ GeV}$, see Fig. 2 for details.

Limits on MLRSM potential parameters have been discussed lately in [11]. Similar to the earlier case we focus on α_3 and $\delta\rho = \rho_3 - 2\rho_1$ parameters, which are important for the scalar mass spectrum (all notations are as in [10, 11]). First, to suppress FCNC effects generated by H_1^0 and A_1^0 , we assume² that their mass is bigger than $M_{\text{FCNC}} = 10 \text{ TeV}$. Because $M_{H_1^0, A_1^0}^2 = \alpha_3 v_R^2/2$, this results in the following lower limit on α_3 :

$$\alpha_3 \geq \frac{2M_{\text{FCNC}}^2}{v_R^2}. \quad (1)$$

Taking into account that $M_{H_1^{\pm\pm}}^2 = (\delta\rho v_R^2 + \alpha_3 \kappa^2)/2$ one gets

$$\alpha_3 \geq \frac{1}{\kappa^2}(2M_{\text{LHC}}^2 - \delta\rho v_R^2), \quad (2)$$

where $\kappa = 246 \text{ GeV}$ is the electroweak symmetry breaking scale. Third constraint originates from the *necessary condition* for the boundedness of the potential [39]:

$$\alpha_3 \leq \sqrt{8\lambda_1(4\pi - \delta\rho)}. \quad (3)$$

The value of λ_1 is fixed by the lightest neutral Higgs boson mass as $M_{H_1^0}^2 = 2\lambda_1\kappa^2$.

² To our knowledge, their effects have been discussed for the first time in the context of Left-Right models in [33], see also [9, 18, 34–36] and recent [37]. In general, their masses need to be at least of the order of 10 TeV, though some alternatives have been also considered in [38].

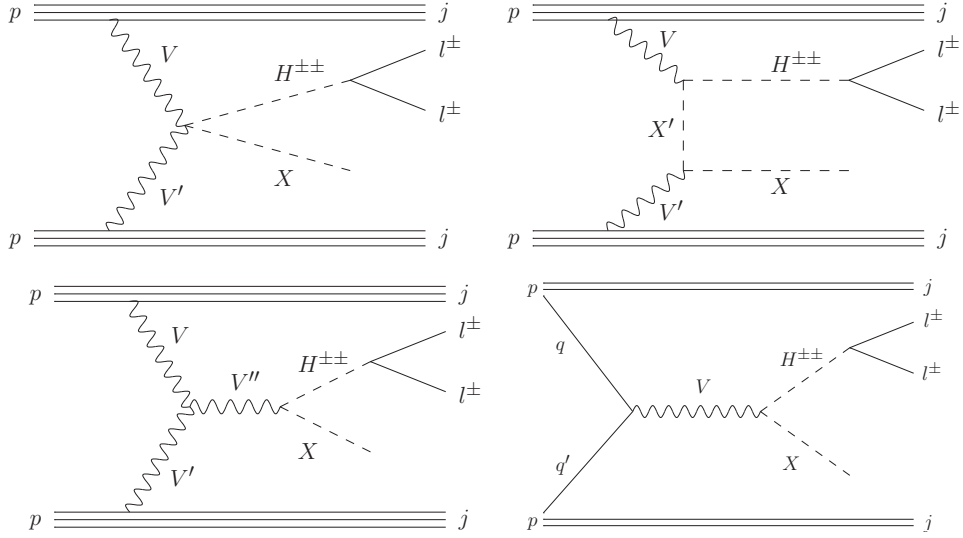


FIG. 1. Basic processes which lead to $H^{\pm\pm}$ pair production. In the first three diagrams $H^{\pm\pm}$ is produced through fusion of two vector bosons V and V' . Each of them can be W^\pm , Z^0 or γ . The second product of the fusion, scalar X , is $H^{\pm\pm}$, H^\pm or H^0 depending on the configuration of colliding vector bosons. Analogously, scalar X' and vector boson V'' can be identified once V and V' are specified. In the last diagram $H^{\pm\pm}$ is produced through collision of two quarks q and q' in the Drell-Yan process. The second product of the decay, scalar X , can be identified as $H^{\pm\pm}$, H^\pm or H^0 once V is specified.

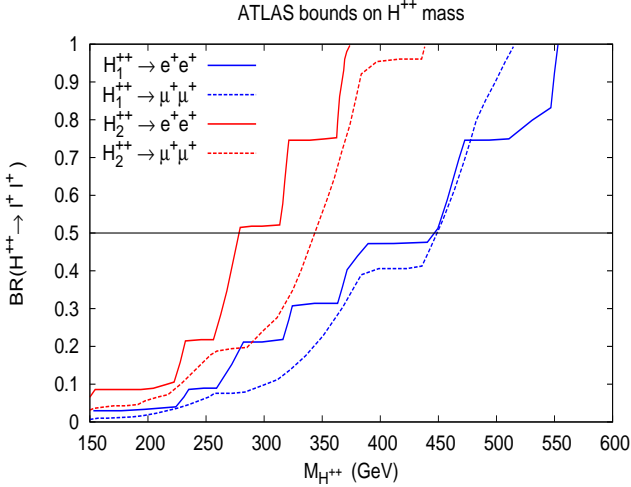


FIG. 2. Exclusion limits on the masses of doubly charged scalars from ATLAS analysis, depending on their leptonic branching ratios. The lepton flavor violating modes are not shown here, as they are not concerned with the purpose of our analysis. This plot is based on Fig. 5 in [32].

Now, it is interesting and important to ask what is the maximum allowed mass splitting $\Delta M = M_{H_1^{\pm\pm}} - M_{H_2^{\pm\pm}}$ that will be consistent with the bounds on $(\alpha_3, \delta\rho)$ derived above. Such queries cannot be unnoticed from phenomenological perspective because only for $\Delta M > M_{W_1^\pm}$, doubly charged Higgs can have following decay: $H_1^{\pm\pm} \rightarrow H_1^\pm W_1^\pm$. Thus, this has a massive impact on decay branching ratios of $H^{\pm\pm}$. It is straightforward to

check that the biggest ΔM is reached for $\delta\rho$ saturating both inequalities in Eqs. (2) and (3) which imply

$$\frac{1}{\kappa^2}(2M_{\text{LHC}}^2 - \delta\rho v_R^2) = \sqrt{8\lambda_1(4\pi - \delta\rho)}. \quad (4)$$

The physical solution to this equation and corresponding maximal value of ΔM is

$$\delta\rho = \frac{2(M_{\text{LHC}}^2 - \sqrt{8\pi\lambda_1}\kappa^2)}{v_R^2}(1 + \dots),$$

$$\Delta M = \Delta M_\infty(1 + \dots), \quad (5)$$

where ‘...’ stands for corrections of the order of $\mathcal{O}(M_{\text{LHC}}^2/v_R^2, \kappa^2/v_R^2)$. One can check that ΔM depends on v_R very weakly and is nearly equal to the asymptotic value $\Delta M_\infty = \lim_{v_R \rightarrow \infty} \Delta M = M_{\text{LHC}} - \sqrt{M_{\text{LHC}}^2 - \sqrt{2\pi\lambda_1}\kappa^2} \approx 65.3 \text{ GeV}$, for $M_{\text{LHC}} = 450 \text{ GeV}$. As $\partial_{v_R} \Delta M > 0$, this implies that on-shell decay $H_1^{\pm\pm} \rightarrow H_1^\pm W_1^\pm$ is kinematically forbidden regardless of the scale v_R . Interestingly, we came to the same conclusion as in [27], but based on different kind of arguments. There is another consequence of the requirement that the scalar potential is bounded from below. Namely, one can show that, using Eqs. (1) and (3), in the allowed parameter space there is an upper limit on $H_1^{\pm\pm}$ mass:

$$M_{H_1^{\pm\pm}} \leq \frac{1}{2} \sqrt{8\pi v_R^2 - \frac{M_{\text{FCNC}}^4}{\lambda_1 v_R^2}}(1 + \dots) \approx 9.98 \text{ TeV}, \quad (6)$$

where ‘...’ stands for the corrections of order of $\mathcal{O}(\kappa^2/v_R^2)$. The maximal value of $M_{H_1^{\pm\pm}}$ is reached

for $\delta\rho$ satisfying $\sqrt{8\lambda_1(4\pi - \delta\rho)} = 2M_{\text{FCNC}}^2/v_R^2$ and $\alpha_3 = 2M_{\text{FCNC}}^2/v_R^2$, which correspond to the intersection point of lines restricting regions defined by Eqs. (1) and (3). The situation is summarized in Fig. 3. Naturally, the minimal value of $H_1^{\pm\pm}$ mass in the discussed setup is M_{LHC} . For the sake of completeness, let us note that if there are no experimental limits on $M_{H_1^{\pm\pm}}$ and H_3^0 then the lowest possible mass of $H_1^{\pm\pm}$ consistent with the vacuum stability bound, Eq. (3), would be $\sqrt{2\sqrt{\pi}}M_{H_3^0}v \approx 330$ GeV, which corresponds to $\delta\rho \rightarrow 0$ and $\alpha_3 \rightarrow \sqrt{32\pi\lambda_1}$. On the other hand, the MLRSM does not provide any relevant constraints on $H_2^{\pm\pm}$ mass³. We would like to mention that when ρ_2 satisfies

$$\rho_2 < \frac{1}{4}\min(\alpha_3, \delta\rho) + \frac{1}{2}\frac{M_{W_{1,2}}^2}{v_R^2} - \frac{1}{8}\alpha_3\frac{\kappa^2}{v_R^2}, \quad (7)$$

then similar type of decay of $H_2^{\pm\pm}$ is kinematically forbidden as $H_2^{\pm\pm}$ is too light to decay into H_2^\pm and $W_{1,2}^\pm$ respectively, see the benchmarks in the next section.

IV. PREDICTIONS FOR

$pp \rightarrow H_{1/2}^{\pm\pm} H_{1/2}^{\mp\mp} jj \rightarrow \ell^\pm \ell^\pm \ell^\mp \ell^\mp jj$ IN MLRSM

Before we discuss our simulated results, selection criteria should be defined, which are crucial for extracting proper signals and reducing the SM background. For selecting leptons we use the same criteria as defined in previous papers [10, 41], which are read as:

- Lepton identification criteria: pseudo-rapidity $|\eta_\ell| < 2.5$ and $p_{T\ell} > 10$ GeV;
- Detector efficiency for charged leptons:
 - electron (either e^\pm): 0.7 (70%);
 - muon (either μ^\pm): 0.9 (90%);
- Smearing of muon p_T and electron energy are implemented in PYTHIA;
- Lepton-lepton separation: $\Delta R_{ll} \geq 0.2$;
- Lepton-photon separation: $\Delta R_{l\gamma} \geq 0.2$ where all the photons have $p_{T\gamma} > 10$ GeV;
- We have implemented Z -veto to suppress the SM background and this has larger impact while reducing the background for four-lepton without missing energy. This veto reads as: Same flavored but opposite sign lepton pair invariant mass $m_{\ell_1\ell_2}$ must be sufficiently away from the SM Z -boson mass, say, $|m_{\ell_1\ell_2} - M_{Z_1}| \geq 6\Gamma_{Z_1} \sim 15$ GeV;

- Lepton-jet separation: The separation of a lepton with all nearby jets must satisfy $\Delta R_{lj} \geq 0.4$. If this is not satisfied then that lepton is not counted as lepton. For completeness, we must mention that jets are constructed from hadrons using PYCELL within the PYTHIA;
- Hadronic activity cut: this cut is applied to consider only those leptons that have very less hadronic activity around them. Each lepton should have hadronic activity which accounted as $\frac{\sum p_{T\text{hadron}}}{p_{Tl}} \leq 0.2$ within the cone of radius 0.2 around the lepton;
- Hard p_T cuts for four lepton events: $p_{Tl_1} > 30$ GeV, $p_{Tl_2} > 30$ GeV, $p_{Tl_3} > 20$ GeV, $p_{Tl_4} > 20$ GeV.

Cuts	p_{Tj_1}, p_{Tj_2}	$ \eta_{j_1} - \eta_{j_2} $	$m_{j_1j_2}$	$\eta_{j_1} * \eta_{j_2}$
VBF	≥ 50	> 4	500	< 0

TABLE I. Selection criteria for the forward jets. The two highest p_T jets p_{Tj_1}, p_{Tj_2} are chosen as the VBF forward jets.

The Parton Distribution Function (PDF) for proton is defined by CTEQ6L1 [42]. After satisfying the above selection criteria, additional cuts are applied to identify the forward jets. The detail of these VBF cuts are depicted in Tab. I.

Taking care of the constraints on potential parameters discussed in section III, in Fig. 4 results are presented for the doubly charged Higgs production process with two jets as a function of their mass. While computing the MLRSM mass spectrum, we have set $v_R = 8$ TeV (which leads to $M_{W_2} = 3.76$ TeV). The analyses are performed for LHC with 14 TeV collision energy considering high luminosity HL-LHC option [43] as well as for future scenarios such as HE-LHC with center of mass energy 33 TeV [43, 44] or 100 TeV FCC-hh facility [45–48]. The cross section for this process has been computed with a large p_{Tj} and VBF cuts as defined in Tab.I

As an example of representative Higgs mass spectrum (bench mark) used in calculations, assuming degenerate doubly charged Higgs masses $M_{H_1^{\pm\pm}} = M_{H_2^{\pm\pm}} = 500$ [1000] GeV where masses of remaining scalar particles compatible with results of section III can be chosen as (in GeV):

$$M_{H_0^0} = 125 [125], M_{H_1^0} = 10431 [10431], \quad (8)$$

$$M_{H_2^0} = 27011 [27011], M_{H_3^0} = 384 [947], \quad (9)$$

$$M_{A_0^0} = 10437 [10437], M_{A_2^0} = 384 [947], \quad (10)$$

$$M_{H_1^\pm} = 446 [974], M_{H_2^\pm} = 10433 [10433]. \quad (11)$$

³ The only constraint which could arise is $M_{H_2^{\pm\pm}} < 2\sqrt{6\pi}v_R \approx 40$ TeV for $v_R = 8$ TeV. It comes from the assumption that scalar potential parameter ρ_2 is in the perturbative regime $\rho_2 < 4\pi$.

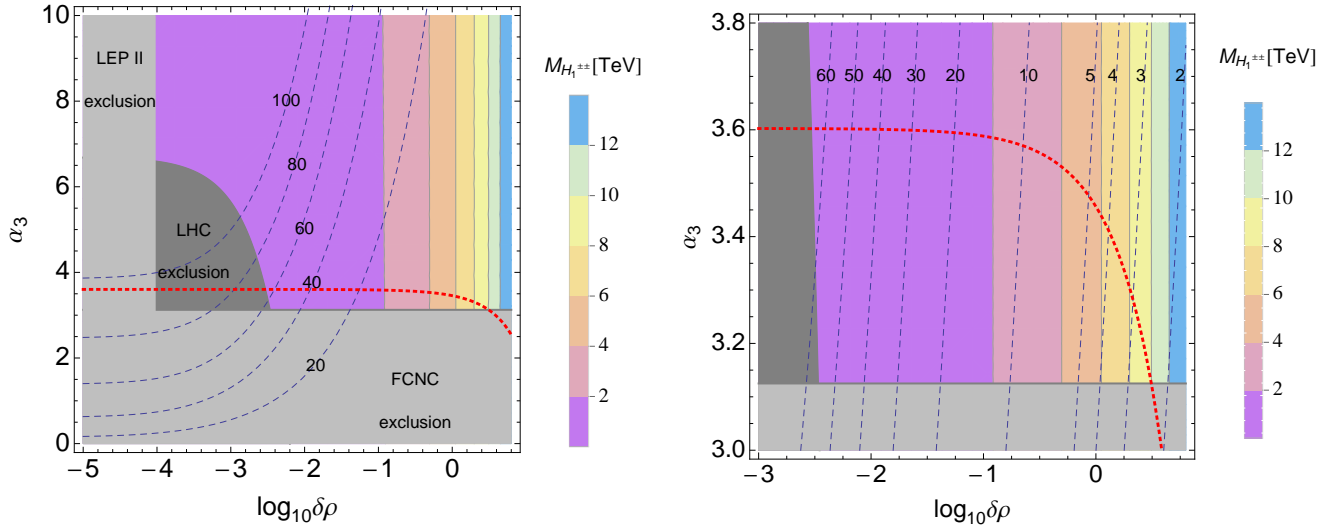


FIG. 3. (*left panel*) Dependence of the $H_1^{\pm\pm}$ mass (in TeV) on $\delta\rho$ and α_3 for $v_R = 8$ TeV. The parameter space $(\delta\rho, \alpha_3)$ is divided into coloured regions where mass of $H_1^{\pm\pm}$ is characterized according to the attached legend. Shaded regions are excluded due to FCNC, LHC and LEP constraints - see Eqs. (1) and (2) and Refs. [11, 40] respectively. The parameter space above the red-dotted line is disfavoured due to the unboundedness of the scalar potential - see Eq. (3). Blue, dashed lines represent sets of points $(\delta\rho, \alpha_3)$ for which mass splitting $(M_{H_1^{\pm\pm}} - M_{H_1^\pm})$ is 100, 80, 60, 40 and 20 GeV respectively. (*right panel*) Detailed view of the allowed part of parameter space with refined mass splitting lines.

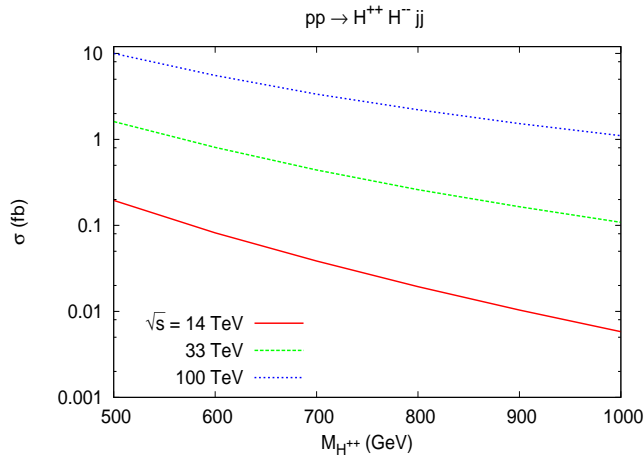


FIG. 4. Dependence of cross sections (σ) with the masses of doubly charged scalars for the process $pp \rightarrow H^{++} H^{-} jj$ for different centre of mass energies: 14 TeV (red-solid), 33 TeV (green-dashed), and 100 TeV (blue-dotted) respectively.

This spectrum is obtained with the following set of potential parameters ($v_R = 8$ TeV):

$$\lambda_1 = 0.129 [0.129], \lambda_2 = 0 [0], \quad (12)$$

$$\lambda_3 = 1 [1] \lambda_4 = 0 [0], \quad (13)$$

$$\alpha_1 = 0 [0], \alpha_2 = 0 [0], \alpha_3 = 3.4 [3.4], \quad (14)$$

$$\rho_1 = 5.7 [5.7], \rho_2 = 0.00115 [0.00701], \quad (15)$$

$$\rho_3 = 11.405 [11.428]. \quad (16)$$

The cross sections for the following process at the parton level with minimal imposed cuts are given as:

$$\begin{aligned} & \sigma(pp \rightarrow H_{1/2}^{\pm\pm} H_{1/2}^{\mp\mp} jj \rightarrow \ell^\pm \ell^\pm \ell^\mp \ell^\mp jj) \quad (17) \\ & = \begin{cases} 4.04 [0.12] \times 10^{-2} \text{ fb} & \text{for } \sqrt{s} = 14 \text{ TeV}, \\ 45.30 [3.36] \times 10^{-2} \text{ fb} & \text{for } \sqrt{s} = 33 \text{ TeV}, \\ 282.80 [31.76] \times 10^{-2} \text{ fb} & \text{for } \sqrt{s} = 100 \text{ TeV}, \end{cases} \end{aligned}$$

where $\ell = e, \mu$. These minimal cuts are e.g. minimum p_T cut for leptons and jets such that they are identified as observable in the detector and do not contribute to missing energy.

The result in Eq. (17) is further processed using the VBF cuts

$$\begin{aligned} & \sigma(pp \rightarrow H_{1/2}^{\pm\pm} H_{1/2}^{\mp\mp} jj \rightarrow \ell^\pm \ell^\pm \ell^\mp \ell^\mp jj) \quad (18) \\ & = \begin{cases} 0.54 [0.01] \times 10^{-2} \text{ fb} & \text{for } \sqrt{s} = 14 \text{ TeV}, \\ 6.21 [0.40] \times 10^{-2} \text{ fb} & \text{for } \sqrt{s} = 33 \text{ TeV}, \\ 37.01 [3.54] \times 10^{-2} \text{ fb} & \text{for } \sqrt{s} = 100 \text{ TeV}. \end{cases} \end{aligned}$$

For the sake of completeness let us display contributions from two intermediate channels⁴ with the default

⁴ In [10] we wrongly assigned $H_1^{\pm\pm}$ with right triplet and $H_2^{\pm\pm}$ with left triplet in Eq. (A.13). We would like to thank Juan Carlos Vasquez for paying our attention to this fact as he considered also this process in [49].

cuts in Madgraph (MG):

$$\begin{aligned} & \sigma(pp \rightarrow H_1^{\pm\pm} H_1^{\mp\mp} jj) \\ & = \begin{cases} 11.16 [0.39] \times 10^{-2} \text{ fb} & \text{for } \sqrt{s} = 14 \text{ TeV,} \\ 90.87 [7.05] \times 10^{-2} \text{ fb} & \text{for } \sqrt{s} = 33 \text{ TeV,} \\ 599.70 [73.28] \times 10^{-2} \text{ fb} & \text{for } \sqrt{s} = 100 \text{ TeV,} \end{cases} \end{aligned} \quad (19)$$

and

$$\begin{aligned} & \sigma(pp \rightarrow H_2^{\pm\pm} H_2^{\mp\mp} jj) \\ & = \begin{cases} 8.35 [0.19] \times 10^{-2} \text{ fb} & \text{for } \sqrt{s} = 14 \text{ TeV,} \\ 71.20 [3.81] \times 10^{-2} \text{ fb} & \text{for } \sqrt{s} = 33 \text{ TeV,} \\ 401.40 [37.43] \times 10^{-2} \text{ fb} & \text{for } \sqrt{s} = 100 \text{ TeV.} \end{cases} \end{aligned} \quad (20)$$

As one can see the cross sections in Eqs. (19) and (20) are larger than these given in Eq. (17). The reason for this is while computing the cross section for leptonic final state, i.e., Eq. (18), all the selection cuts are incorporated and that reduces the cross section by a large amount.

Some technical details related to computing method are in order here. At the MG level one can control gluons contributions using option `QCD=0`. The cross section for $pp \rightarrow H_{1,2}^{\pm\pm} H_{1,2}^{\mp\mp} jj$ with switched off gluons turns out to be about 5 times smaller than that for with gluons. Hence QCD contributions to that signal are really important. However, in both cases distributions of rapidity (y) of jets are quite different. Allowing for gluons they are peaked around $y = 0$ which implies that jets are emitted mostly perpendicular to the beam, otherwise rapidities are peaked around $|y| \sim 3$ and $|y_1 - y_2| \sim 5$, i.e. there are two back-to-back jets emitted along the beam. Hence setting `QCD=0` allows us to preselect processes which are consistent with VBF cuts. Effectively it shortens computing time⁵.

Let us comment on the $H^{\pm\pm}$ decay scenario used in calculations. It is assumed that the decay of $H^{\pm\pm}$ is dominantly into a pair of the same sign same flavored charged leptons (for all possibilities within MLRSM, see [10]). In other words, it is assumed that Yukawa coupling matrix of doubly charged scalar $H_2^{\pm\pm}$ with charged leptons is diagonal. Assuming no mixed leptonic decay modes ($e\mu$), i.e., no lepton flavor violation, the coupling of doubly charged scalar $H_2^{\pm\pm}$ with charged leptons in MLRSM is proportional to the heavy neutrino mass of the corresponding lepton generation. Thus the $ee, \mu\mu$ decay modes will be larger compare to the $\tau\tau$ case if the first and second generations of right handed neutrinos are more massive than the third generation one. This point has been clarified and shown numerically in Fig. 2.5 in Ref. [10]. In the present analysis the masses of the first two generations of right handed neutrinos are taken to be 3 TeV and mass of the third one is at the level of 800 GeV.

As $v_R = 8$ TeV, the Yukawa couplings are within the perturbative limit. If the $\tau\tau$ decay mode would be larger, predictions given here should be rescaled properly using corresponding branching ratios (for instance, in the democratic three generation case, branching ratio for the ee and $\mu\mu$ channels would be decreased by about 15%, each).

Process: $ZZjj$ with \sqrt{s} in TeV	Cross section [fb] at parton level in Madgraph	Cross section [fb] after showering, and hadronization in PYTHIA
14	0.115	0.003
33	1.109	0.008
100	4.794	0.038

TABLE II. Standard Model cross section in fb for $\ell^+ \ell^- \ell^+ \ell^- jj$ final state and $\sqrt{s} = 14, 33, 100$ TeV LHC. The cuts are suitably applied, see section IV, to compute the SM background at parton level and after incorporating showering and hadronization in PYTHIA.

The SM background at the LHC for the signal $4\ell + 2$ jets is accounted from the process $pp \rightarrow ZZ(\gamma\gamma, Z\gamma)jj \rightarrow \ell^+ \ell^- \ell^+ \ell^- jj$. We have noted that after implementation of the selection cuts the dominant background is contributed from $pp \rightarrow ZZjj \rightarrow \ell^+ \ell^- \ell^+ \ell^- jj$ process.

For $\sqrt{s} = 14, 33, 100$ TeV pp collisions, the SM background is given in Tab. II both at the parton level and after hadronization and passing through implemented cuts.

We can see that the background is suppressed very effectively. The results in Tab. II are obtained in the leading order, electroweak corrections can change the results not more than 10% [50] which can change the significance of signals at the level of about one percent at most.

Finally, to judge the strength of the MLRSM signals we decided to show the dependence of the significance of the result as a function of the integrated luminosity. As can be seen in Fig. 5 (left-top), a comfortable value of the significance at the level of 5 can be reached for $M_{H^{\pm\pm}} = 500$ GeV in pp collisions with

- $\sqrt{s} = 100$ TeV and with 100 fb^{-1} integrated luminosity;
- $\sqrt{s} = 33$ TeV and with 700 fb^{-1} integrated luminosity.

No signal at this significance level (~ 5) can be reached with $\sqrt{s} = 14$ TeV pp collisions, even if the integrated luminosity is around 3000 fb^{-1} .

In Fig. 5 (right-top) we can see that doubly charged Higgs bosons with masses up to $M_{H^{\pm\pm}} = 700$ GeV with significance at the level of 5 can be probed for both center of mass energy 33 and 100 TeV with integrated luminosities around 3000 and 300 fb^{-1} respectively. In Fig. 5 (left-bottom) it is evident that 1 TeV doubly charged scalar can be probed with significance of 5 only with 100 TeV collider with luminosity at least 1000 fb^{-1} . The Fig. 5

⁵ Typical run times for generating $5 \cdot 10^4$ events of $pp \rightarrow H_{1/2}^{\pm\pm} H_{1/2}^{\mp\mp} jj$ and $pp \rightarrow H_{1/2}^{\pm\pm} H_{1/2}^{\mp\mp} jj \rightarrow \ell^\pm \ell^\pm \ell^\mp \ell^\mp jj$ with `QCD=0` are, respectively, about 3 h and 54 h on 8 core 3.4 GHz CPU.

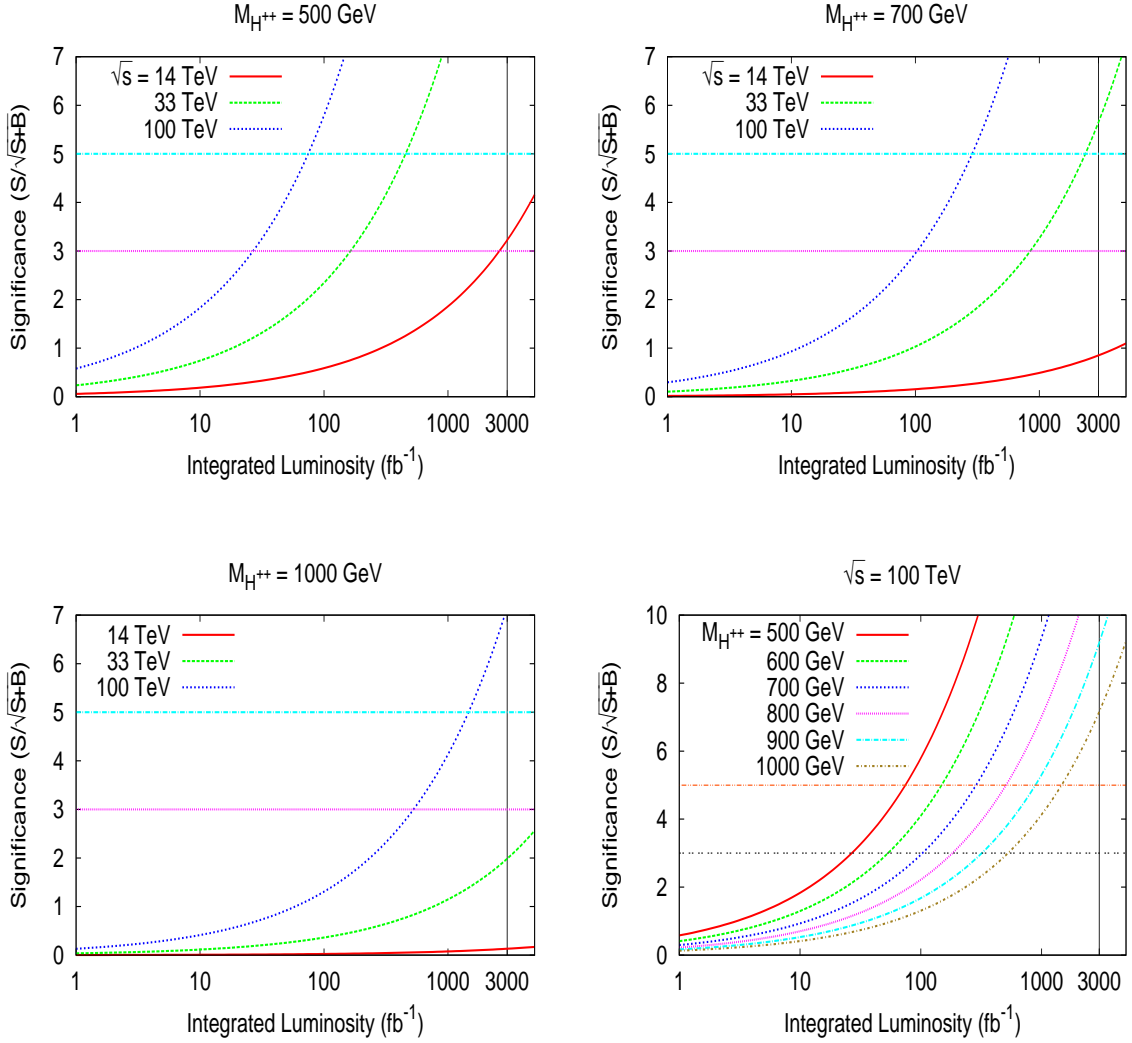


FIG. 5. Variations of significance of *signal* with integrated luminosities for different energies of pp colliders and various doubly charged Higgs boson masses.

(right-bottom) summarizes situation for the FCC-hh collider option for three different set of masses of doubly charged scalars: 500, 600, 700, 800, 900 and 1000 GeV. This figure also shows that significance at the level of 7 can be reached for $M_{H^{\pm\pm}} = 1 \text{ TeV}$ and $\sqrt{s} = 100 \text{ TeV}$ with integrated luminosities around 3000 fb^{-1} . We can see that this collider opens up very wide range of Higgs boson masses which can be explored.

V. CONCLUSIONS AND OUTLOOK

In this paper we have considered production and decays of pair of doubly charged Higgs bosons through vector boson fusion within MLRSM framework. To do so we have evaluated suitable bench mark points for masses of Higgs bosons, which are in agreement with several constraints coming from FCNC, vacuum stability, LEP II and

recent ATLAS searches on doubly charged scalars. There are strong relations among masses of doubly, singly and neutral scalars which forbid us to choose their individual values freely, leaving us with suitable benchmarks we are using in this paper. We have further noted and shown that the splitting between the doubly ($H_1^{\pm\pm}$) and singly (H_1^\pm) charged scalars is less than M_{W_1} , irrespective of the $SU(2)_R$ breaking scale. Thus the on-shell decay $H_1^{\pm\pm} \rightarrow H_1^\pm W_1^\pm$ is protected and the decay branching ratio of the doubly charged scalar $H_1^{\pm\pm}$ is affected.

After settling these issues regarding the spectrum we have computed the signal cross section for the process $pp \rightarrow H_{1/2}^{\pm\pm} H_{1/2}^{\mp\mp} jj \rightarrow \ell^\pm \ell^\pm \ell^\mp \ell^\mp jj$ using realistic cuts. The necessary SM background for this final state is also evaluated. It has been shown that LHC2 even with high integrated luminosity will be not be sensitive to the VBF-like signals $H_{1/2}^{\pm\pm} H_{1/2}^{\mp\mp} jj$, even with relatively light doubly

charged Higgs bosons (say, ~ 500 GeV). We have shown much better perspective exists for the future FCC colliders with center of mass energies 33 and (or) 100 TeV.

In passing we would like to mention that we have used the VBF cuts as adopted in [27]. We have compared the ATLAS and CMS (tight & loose) suggested cuts which are not very widely different from significance point of view.

Let us conclude with a comparative comment: MLRSM VBF-like signals connected with $H_2^{\pm\pm}$ scalar production (which is a part of the right handed triplet) is comparable with the $H_1^{\pm\pm}$ scalar production, see Eqs. (19) and (20). Thus the cross section for signal events are larger compare to that for Type-II seesaw scenario with same masses for triplet scalars. It may give a chance to disentangle between MLRSM and SM with

additional triplet, e.g. Higgs Triplet Model [19, 51–55], though detailed analyses are needed to compare.

ACKNOWLEDGEMENTS

The authors would like to thank Benjamin Fuks for sharing with them modified version of FeynRules. Work is supported by the Department of Science & Technology, Government of India under the Grant Agreement No. IFA12-PH-34 (INSPIRE Faculty Award) and Polish National Science Centre (NCN) under the Grant Agreement No. DEC-2013/11/B/ST2/04023 and under post-doctoral grant No. DEC-2012/04/S/ST2/00003. Work of RS is supported by Science and Engineering Research Canada (NSERC).

-
- [1] R. Cahn and S. Dawson, *Production of Very Massive Higgs Bosons*, *Phys.Lett.* **B136** (1984) 196.
- [2] D. L. Rainwater and D. Zeppenfeld, *Searching for $H \rightarrow \gamma\gamma$ in weak boson fusion at the LHC*, *JHEP* **9712** (1997) 005, [[hep-ph/9712271](#)].
- [3] D. L. Rainwater, D. Zeppenfeld, and K. Hagiwara, *Searching for $H \rightarrow \tau^+\tau^-$ in weak boson fusion the CERN LHC*, *Phys.Rev.* **D59** (1998) 014037, [[hep-ph/9808468](#)].
- [4] K. Kawade, O. Adriani, L. Bonechi, M. Bongi, G. Castellini, et al., *The performance of the LHCf detector for hadronic showers*, *JINST* **9** (2014) P03016, [[arXiv:1312.5950](#)].
- [5] **FP420 R and D** Collaboration, M. Albrow et al., *The FP420 & Project: Higgs and New Physics with forward protons at the LHC*, *JINST* **4** (2009) T10001, [[arXiv:0806.0302](#)].
- [6] P. J. Fox, R. Harnik, J. Kopp, and Y. Tsai, *Missing Energy Signatures of Dark Matter at the LHC*, *Phys.Rev.* **D85** (2012) 056011, [[arXiv:1109.4398](#)].
- [7] **ATLAS** Collaboration, *Search for New Phenomena in Monojet plus Missing Transverse Momentum Final States using 10fb-1 of pp Collisions at $\sqrt{s}=8$ TeV with the ATLAS detector at the LHC*, .
- [8] **CMS** Collaboration, V. Khachatryan et al., *Search for dark matter, extra dimensions, and unparticles in monojet events in proton-proton collisions at $\sqrt{s} = 8$ TeV*, [arXiv:1408.3583](#).
- [9] J. Chakraborty, J. Gluza, R. Sevilano, and R. Szafron, *Left-Right Symmetry at LHC and Precise 1-Loop Low Energy Data*, *JHEP* **1207** (2012) 038, [[arXiv:1204.0736](#)].
- [10] G. Bambhaniya, J. Chakraborty, J. Gluza, M. Kordiaczyńska, and R. Szafron, *Left-Right Symmetry and the Charged Higgs Bosons at the LHC*, *JHEP* **1405** (2014) 033, [[arXiv:1311.4144](#)].
- [11] G. Bambhaniya, J. Chakraborty, J. Gluza, T. Jeliński, and M. Kordiaczyńska, *Lowest limits on the doubly charged Higgs boson masses in the minimal left-right symmetric model*, *Phys.Rev.* **D90** (2014), no. 9 095003, [[arXiv:1408.0774](#)].
- [12] R. Mohapatra and J. C. Pati, *A Natural Left-Right Symmetry*, *Phys.Rev.* **D11** (1975) 2558.
- [13] G. Senjanovic and R. N. Mohapatra, *Exact Left-Right Symmetry and Spontaneous Violation of Parity*, *Phys.Rev.* **D12** (1975) 1502.
- [14] R. Mohapatra, *Unification and Supersymmetry. The Frontiers of Quark-Lepton Physics*, Springer 1986, .
- [15] R. N. Mohapatra and G. Senjanovic, *Neutrino Masses and Mixings in Gauge Models with Spontaneous Parity Violation*, *Phys.Rev.* **D23** (1981) 165.
- [16] J. Gunion, J. Grifols, A. Mendez, B. Kayser, and F. I. Olness, *Higgs Bosons in Left-Right Symmetric Models*, *Phys.Rev.* **D40** (1989) 1546.
- [17] P. Duka, J. Gluza, and M. Zralek, *Quantization and renormalization of the manifest left-right symmetric model of electroweak interactions*, *Annals Phys.* **280** (2000) 336–408, [[hep-ph/9910279](#)].
- [18] Y. Zhang, H. An, X. Ji, and R. N. Mohapatra, *General CP Violation in Minimal Left-Right Symmetric Model and Constraints on the Right-Handed Scale*, *Nucl.Phys.* **B802** (2008) 247–279, [[arXiv:0712.4218](#)].
- [19] A. Melfo, M. Nemevsek, F. Nesti, G. Senjanovic, and Y. Zhang, *Type II Seesaw at LHC: The Roadmap*, *Phys.Rev.* **D85** (2012) 055018, [[arXiv:1108.4416](#)].
- [20] **CMS** Collaboration, V. Khachatryan et al., *Search for heavy neutrinos and W bosons with right-handed couplings in proton-proton collisions at $\sqrt{s} = 8$ TeV*, [arXiv:1407.3683](#).
- [21] N. D. Christensen and C. Duhr, *FeynRules - Feynman rules made easy*, *Comput.Phys.Commun.* **180** (2009) 1614–1641, [[arXiv:0806.4194](#)].
- [22] C. Degrande, C. Duhr, B. Fuks, D. Grellscheid, O. Mattelaer, et al., *UFO - The Universal FeynRules Output*, *Comput.Phys.Commun.* **183** (2012) 1201–1214, [[arXiv:1108.2040](#)].
- [23] M. L. Mangano, M. Moretti, F. Piccinini, R. Pittau, and A. D. Polosa, *ALPGEN, a generator for hard multiparton processes in hadronic collisions*, *JHEP* **0307** (2003) 001, [[hep-ph/0206293](#)].
- [24] J. Alwall, M. Herquet, F. Maltoni, O. Mattelaer, and T. Stelzer, *MadGraph 5 : Going Beyond*, *JHEP* **1106** (2011) 128, [[arXiv:1106.0522](#)].
- [25] T. Sjostrand, S. Mrenna, and P. Z. Skands, *PYTHIA 6.4 Physics and Manual*, *JHEP* **0605** (2006) 026,

- [hep-ph/0603175].
- [26] CMS Collaboration, A. Massironi, *VBS/VBF from CMS*, arXiv:1409.2990.
- [27] B. Dutta, R. Eusebi, Y. Gao, T. Ghosh, and T. Kamon, *Exploring the Doubly Charged Higgs of the Left-Right Symmetric Model using Vector Boson Fusion-like Events at the LHC*, *Phys.Rev.* **D90** (2014) 055015, [arXiv:1404.0685].
- [28] C. Englert, E. Re and M. Spannowsky, *Pinning down Higgs triplets at the LHC*, *Phys. Rev.* **D88** (2013) 035024 [arXiv:1306.6228].
- [29] M. Czakon, M. Zralek, and J. Gluza, *Left-right symmetry and heavy particle quantum effects*, *Nucl.Phys.* **B573** (2000) 57–74, [hep-ph/9906356].
- [30] M. Czakon, J. Gluza, F. Jegerlehner, and M. Zralek, *Confronting electroweak precision measurements with new physics models*, *Eur.Phys.J.* **C13** (2000) 275–281, [hep-ph/9909242].
- [31] M. Czakon, J. Gluza, and J. Hejczyk, *Muon decay to one loop order in the left-right symmetric model*, *Nucl.Phys.* **B642** (2002) 157–172, [hep-ph/0205303].
- [32] ATLAS Collaboration, G. Aad et al., *Search for anomalous production of prompt same-sign lepton pairs and pair-produced doubly charged Higgs bosons with $\sqrt{s} = 8$ TeV pp collisions using the ATLAS detector*, arXiv:1412.0237.
- [33] G. Ecker, W. Grimus, and H. Neufeld, *Higgs Induced Flavor Changing Neutral Interactions in $SU(2)_l \times SU(2)_r \times U(1)$* , *Phys.Lett.* **B127** (1983) 365.
- [34] R. N. Mohapatra, G. Senjanovic, and M. D. Tran, *Strangeness Changing Processes and the Limit on the Right-handed Gauge Boson Mass*, *Phys.Rev.* **D28** (1983) 546.
- [35] M. Pospelov, *FCNC in left-right symmetric theories and constraints on the right-handed scale*, *Phys.Rev.* **D56** (1997) 259–264, [hep-ph/9611422].
- [36] A. Maiezza, M. Nemevsek, F. Nesti, and G. Senjanovic, *Left-Right Symmetry at LHC*, *Phys.Rev.* **D82** (2010) 055022, [arXiv:1005.5160].
- [37] S. Bertolini, A. Maiezza, and F. Nesti, *Present and Future K and B Meson Mixing Constraints on TeV Scale Left-Right Symmetry*, *Phys.Rev.* **D89** (2014), no. 9 095028, [arXiv:1403.7112].
- [38] D. Guadagnoli and R. N. Mohapatra, *TeV Scale Left Right Symmetry and Flavor Changing Neutral Higgs Effects*, *Phys.Lett.* **B694** (2011) 386–392, [arXiv:1008.1074].
- [39] J. Chakraborty, P. Konar, and T. Mondal, *Copositive Criteria and Boundedness of the Scalar Potential*, *Phys.Rev.* **D89** (2014) 095008, [arXiv:1311.5666].
- [40] A. Datta and A. Raychaudhuri, *Mass bounds for triplet scalars of the left-right symmetric model and their future detection prospects*, *Phys.Rev.* **D62** (2000) 055002, [hep-ph/9905421].
- [41] G. Bambhaniya, J. Chakraborty, S. Goswami, and P. Konar, *Generation of Neutrino mass from new physics at TeV scale and Multi-lepton Signatures at the LHC*, arXiv:1305.2795.
- [42] J. Pumplin, D. Stump, J. Huston, H. Lai, P. M. Nadolsky, et al., *New generation of parton distributions with uncertainties from global QCD analysis*, *JHEP* **0207** (2002) 012, [hep-ph/0201195].
- [43] W. Barletta, M. Battaglia, M. Klute, M. Mangano, S. Prestemon, et al., *Working Group Report: Hadron Colliders*, arXiv:1310.0290.
- [44] R. Assmann, R. Bailey, O. Brüning, O. Dominguez Sanchez, G. de Rijk, J. M. Jimenez, S. Myers, L. Rossi, L. Tavian, E. Todesco, and F. Zimmermann, *First Thoughts on a Higher-Energy LHC*, Tech. Rep. CERN-ATS-2010-177, CERN, Geneva, Aug, 2010.
- [45] *Future Circular Collider*, <http://cern.ch/fcc>.
- [46] *FCC on CERN Document Server*, <http://cds.cern.ch/collection/FutureCircularColliderDocuments>.
- [47] F. Z. Johannes Gutleber, Michael Benedikt, *Study Brief February 2015*, <http://cds.cern.ch/record/1994232/>.
- [48] *FCC Week 2015*, <http://indico.cern.ch/event/340703/>.
- [49] J. C. Vasquez, *Right-handed lepton mixings at the LHC*, arXiv:1411.5824.
- [50] S. Catani, L. Cieri, G. Ferrera, D. de Florian, and M. Grazzini, *Vector boson production at hadron colliders: a fully exclusive QCD calculation at NNLO*, *Phys.Rev.Lett.* **103** (2009) 082001, [arXiv:0903.2120].
- [51] T. Han, B. Mukhopadhyaya, Z. Si and K. Wang, *Pair production of doubly-charged scalars: Neutrino mass constraints and signals at the LHC*, *Phys. Rev.* **D76** (2007) 075013 [arXiv:0706.0441].
- [52] P. Fileviez Perez, T. Han, G. y. Huang, T. Li and K. Wang, *Neutrino Masses and the CERN LHC: Testing Type II Seesaw*, *Phys. Rev.* **D78** (2008) 015018 [arXiv:0805.3536].
- [53] C. Englert, E. Re and M. Spannowsky, *Triplet Higgs boson collider phenomenology after the LHC*, *Phys. Rev.* **D87** (2013) 9, 095014 [arXiv:1302.6505].
- [54] Z. Kang, J. Li, T. Li, Y. Liu, and G.-Z. Ning, *Light Doubly Charged Higgs Boson via the Di-W Channel at LHC*, arXiv:1404.5207.
- [55] S. Kanemura, M. Kikuchi, K. Yagyu, and H. Yokoya, *Bounds on the mass of doubly-charged Higgs bosons in the same-sign diboson decay scenario*, *Phys.Rev.* **D90** (2014), no. 11 115018, [arXiv:1407.6547].